BIBLIOGRAPHIC INFORMATION SYSTEM

JOURNAL FULL TITLE: Journal of Biomedical Research & Environmental Sciences
ABBREVIATION (NLM): J Biomed Res Environ Sci **ISSN:** 2766-2276 **WEBSITE:** https://www.jelsciences.com

SCOPE & COVERAGE

- **Sections Covered:** 34 specialized sections spanning 143 topics across Medicine, Biology, Environmental Sciences, and General Science
- Ensures broad interdisciplinary visibility for high-impact research.

PUBLICATION FEATURES

- **Review Process:** Double-blind peer review ensuring transparency and quality
- **Time to Publication:** Rapid 21-day review-to-publication cycle
- **Frequency:** Published monthly
- **Plagiarism Screening:** All submissions checked with iThenticate

INDEXING & RECOGNITION

- **Indexed in:** Google Scholar, IndexCopernicus (**ICV 2022: 88.03**)
- **DOI:** Registered with CrossRef (**10.37871**) for long-term discoverability
- **Visibility:** Articles accessible worldwide across universities, research institutions, and libraries

OPEN ACCESS POLICY

- Fully Open Access journal under Creative Commons Attribution 4.0 License (CC BY 4.0)
- Free, unrestricted access to all articles globally

GLOBAL ENGAGEMENT

- **Research Reach:** Welcomes contributions worldwide
- **Managing Entity:** SciRes Literature LLC, USA
- **Language of Publication:** English

SUBMISSION DETAILS

- Manuscripts in Word (.doc/.docx) format accepted

SUBMISSION OPTIONS

- **Online:** https://www.jelsciences.com/submit-your-paper.php
- **Email:** support@jelsciences.com, support@jbresonline.com

HOME ABOUT ARCHIVE SUBMIT MANUSCRIPT APC

Vision: The Journal of Biomedical Research & Environmental Sciences (JBRES) is dedicated to advancing science and technology by providing a global platform for innovation, knowledge exchange, and collaboration. Our vision is to empower researchers and scientists worldwide, offering equal opportunities to share ideas, expand careers, and contribute to discoveries that shape a healthier, sustainable future for humanity.

JOURNAL OF BIOMEDICAL RESEARCH & ENVIRONMENTAL SCIENCES
ISSN: 2766-2276
SUBJECT AREA(S): ONCOLOGY | NANOMEDICINE
DOI: 10.37871

RESEARCH ARTICLE

Improved Anticancer Activity of Paclitaxel *via* Folic Acid-Mediated Chitosan Nanoparticles

Pooja KM[1], Patra A[1], Agrawal R[1], Maru S[2], Rajpoot K[3] and Jain SK[1]*

[1]Department of Pharmacy, Guru Ghasidas Vishwavidyalaya, Bilaspur, Chhattisgarh-495 009, India
[2]Department of Pharmacology, School of Pharmacy and Technology Management, NMIMS, Shirpur, India
[3]Babulal Tarabai Institute of Pharmaceutical Sciences, BTIPS, Sironja, Sagar, Madhya Pradesh, India

Abstract

Purpose: Colorectal Cancer (CRC) is among the most prevalent malignancies of the gastrointestinal tract. Globally, it ranks as the third most frequently diagnosed cancer and the second leading cause of cancer-associated mortality. The objective of the research work was to develop a formulation with improved targeting characteristics for the efficient treatment of CRC. Thus, Folic Acid (FA) functionalized Paclitaxel (PAC) loaded Chitosan (CH) Nanoparticles (FA-CH-PAC-NPs) were developed and characterized.

Methods: The ionic gelation process was employed to develop Chitosan Nanoparticles (CH-NPs), which were then conjugated with FA utilizing the carbodiimide chemistry approach. Size of particles, surface structure, drug entrapment efficiency, and zeta potential are some of the critical factors that were taken into consideration when evaluating the formulations and optimizing them for different process variables. Furthermore, the MCF-7 cell line was used to assess In vitro cytotoxicity of improved formulations.

Results: The optimized FA-conjugated formulations exhibited an average particle size and zeta potential of 299 nm and 4.9 mV, respectively, and the drug entrapment efficiency was an excellent 83.5%. Eventually, the % PAC released from pure PAC, CH-PAC-NPs, and FA-CH-PAC-NPs was found to be 97.20%, 57.65%, and 68.88%, respectively, after a 24 h study period. The IC50 values, representing the concentration at which 50% of cell growth is inhibited, were 135.74 ± 0.053 µg/ml for PAC and significantly lower at 42.72 ± 0.132 µg/ml for FA-CH-PAC-NPs.

Conclusion: The results suggest that the optimized formulation FA-CH-PAC-NPs would have improved anticancer effects as well as targeting capability for the management of CRC.

***Corresponding author(s)**

Jain SK, Department of Pharmacy, Guru Ghasidas Vishwavidyalaya, Bilaspur (C.G.) 495 009, India

Email: suniljain25in@yahoo.com

DOI: 10.37871/jbres2246

Submitted: 12 December 2025

Accepted: 29 December 2025

Published: 30 December 2025

Keywords

- Anticancer drugs
- Nanoparticles
- Paclitaxel
- Colon cancer
- Folic acid
- Chitosan

Scan Me

How to cite this article: Pooja KM, Patra A, Agrawal R, Maru S, Rajpoot K, Jain SK. Improved Anticancer Activity of Paclitaxel *via* Folic Acid-Mediated Chitosan Nanoparticles. J Biomed Res Environ Sci. 2025 Dec 30; 6(12): 2002-2016. doi: 10.37871/jbres2246, Article ID: JBRES2246, Available at: https://www.jelsciences.com/articles/jbres2246.pdf

Introduction

Colorectal Cancer (CRC) is caused by mutations that target Deoxyribonucleic Acid (DNA) repair systems, oncogenes, and tumor suppressor genes. Studies suggest that 70% of CRC are sporadic, while 5% are inherited, and 25% of CRC are familial [1,2].

Colorectal Cancer (CRC) represents the third most frequently detected neoplasm and the second foremost contributor to cancer-associated deaths globally, accounting for approximately 1.9 million newly reported cases and nearly 0.9 million fatalities in 2022 [3,4]. Although incidence rates have stabilized or declined in high-income countries due to effective screening and lifestyle modifications. A sharp increase is observed in Asia, Latin America, and Africa, driven by urbanization, dietary shifts, obesity, and sedentary lifestyles [5,6]. Colorectal cancer stands as the fourth most diagnosed cancer in India, with 64,863 recently reported cases and 38,367 associated mortalities in 2022. A growing concern is the rise in early-onset CRC (< 50 years), projected to constitute up to 23% of rectal cancers by 2030 [7,8]. Risk factors include red meat consumption, alcohol, tobacco, obesity, and diabetes, whereas high-fiber diets, legumes, and physical activity confer protection. Hence, the increased prevalence and high mortality rate of CRC demand an urgent need for novel treatment options.

CRC therapy is limited by systemic toxicity and poor bioavailability of conventional drugs. Colon-Targeted Drug Delivery Systems (CTDDS) have been developed to release drugs specifically in the colon, reducing premature degradation and adverse effects in the upper gastrointestinal tract [9-12]. These systems exploit colonic physiology, including pH variation, prolonged transit, and microbial enzymes capable of degrading polysaccharides and azo linkages [13-16]. CTDDS enables localized and sustained delivery of agents like 5-fluorouracil, capecitabine, and phytoconstituents, improving therapeutic outcomes [17]. Approaches include pH-sensitive polymers, time-dependent systems, and microbiota-triggered carriers using chitosan, pectin, and guar gum [18]. CTDDS thus represents a promising strategy for personalized CRC therapy.

CRC therapy has increasingly turned toward nanotechnology-based approaches to overcome the limitations of conventional chemotherapy. Among natural polymers, Chitosan (CH) has attracted particular interest. Its cationic nature, due to protonated amine groups, allows CH to interact electrostatically with negatively charged mucosal surfaces, thereby prolonging residence time in the gastrointestinal tract [19]. Moreover, CH can transiently open epithelial tight junctions, improving paracellular transport and drug absorption. These properties, combined with its biodegradability and safety profile, make CH an excellent carrier for oral delivery of anticancer agents, peptides, and nucleic acids [20-22].

Nanoparticles (NPs) could be altered using targeted ligands, including polysaccharides, transferrins, and integrins, as well as Folic Acid (FA). This modification improves their targeting ability and enhances the internalization of NPs in target tissues to deliver the drug. The surface of cancer cells exhibits high expression of folate receptors when compared to normal tissues, which makes them ideal for tumor-specific drug delivery. To improve the NPs' targeting ability towards tumor cells and boost the drug's antitumor effect, FA is widely employed [23-25].

Building on this mucoadhesive platform, functionalization with targeting ligands further enhances specificity. Among these, Folic Acid (FA) has become a prominent choice because its receptor (FR-α) is overexpressed in several malignancies, including CRC. Elevated FR-α expression not only correlates with tumor invasiveness but also predicts poor prognosis, making it a clinically relevant target for drug delivery. Functionalizing chitosan-based

nanoparticles with FA improves selective uptake by cancer cells, ensuring higher drug accumulation in tumors while sparing healthy tissues [26].

One therapeutic agent that particularly benefits from such strategies is Paclitaxel (PAC). Despite being an important chemotherapeutic that stabilizes microtubules and induces apoptosis, its clinical use is limited by poor solubility and severe toxicities. These toxicities are associated with its solvent-based formulation (Taxol®), which contains Cremophor EL and ethanol. To mitigate these drawbacks, albumin-bound nanoparticle formulations (Abraxane®) have been developed, eliminating Cremophor EL and improving tumor bioavailability. When integrated into colon-targeted and FA-modified chitosan nanoparticle systems, PAC delivery can be further optimized-enhancing solubility, reducing systemic toxicity, and exploiting tumor-specific FR-mediated uptake for improved therapeutic outcomes in CRC [27,28].

To lessen the off-target effects on normal healthy cells of traditional chemotherapy, this research intends to develop and evaluate the PAC-loaded CH-NPs. The research then engineers them with FA for targeting cancer cells overexpressed with folate receptors in the colon region to effectively treat CRC. In detail, FA-conjugated CH-NPs were aimed to target CRC cells specifically owing to their significantly high affinity towards excessively expressed folate receptors. Schematic strategy of drug targeting of designed formulations is shown in figure 1. This novel approach will not only reduce wastage of high-cost anticancer drugs but also reduce toxicity on normal healthy cells.

Materials and Methods

Materials

A complimentary sample of Paclitaxel (≥ 99% pure) was given by Fresenius Kabi Oncology Ltd. (Gurgaon, Haryana). Chitosan (Low molecular weight, > 75% deacetylated) and Sodium Tripolyphosphate (STPP) were purchased from CDH Fine Chemicals, New Delhi. Acetic acid, sodium hydroxide, and Folic Acid (FA) (≥ 98% pure) were obtained from Central Drug House Pvt. Ltd. (Darya Ganj, Delhi, India). Sigma Chemicals (Sydney, Australia) supplied the 1-ethyl-3-(3-dimethylaminopropyl) carbodiimide hydrochloride (EDC).

Synthesis of FA-CH conjugates: FA-CH conjugates were synthesized using the carbodiimide chemistry technique (Figure 2) [29]. In brief, 1.0 g of Chitosan (CH) was solubilized in 100 mL of 1% acetic acid solution. Folic Acid (FA) and EDC were dissolved separately in anhydrous Dimethyl Sulfoxide (DMSO) to obtain a mixed solution. This solution was then added dropwise into the CH solution under continuous magnetic stirring (GI 631, ELICO, India) at different temperatures. The reaction mixture was allowed to stand for a predetermined time, after which 300 mL of acetone was added to induce coagulation. The product was subsequently dialyzed against DMSO for two days, followed by thorough washing with distilled water. Finally, the obtained yellow-colored FA–CH conjugates were freeze-dried (Macro Scientific Works, India) for 24 h at 50˚C.

Preparation of CH-PAC-NPs and FA-CH-PAC-NPs: The polymer (CH/FA-CH, 1.2 mg/mL) was dissolved in a 1% acetic acid solution and subjected to continuous stirring for 24 hours. Sodium Tripolyphosphate (STPP) solution (0.9 mg/mL) was prepared separately in distilled water, in which paclitaxel (PAC, 50 mg) was dissolved. The STPP solution was filtered, and 4 mL of this solution was added dropwise, using a 22-gauge syringe, into 10 mL of the polymer solution under continuous magnetic stirring (1500 rpm) at room temperature (Remi Service Pvt. Ltd., Mumbai, India). The mixture was subjected to continuous stirring for 2 hours to facilitate crosslinking. Thereafter, the nanoparticle dispersion was left to stand

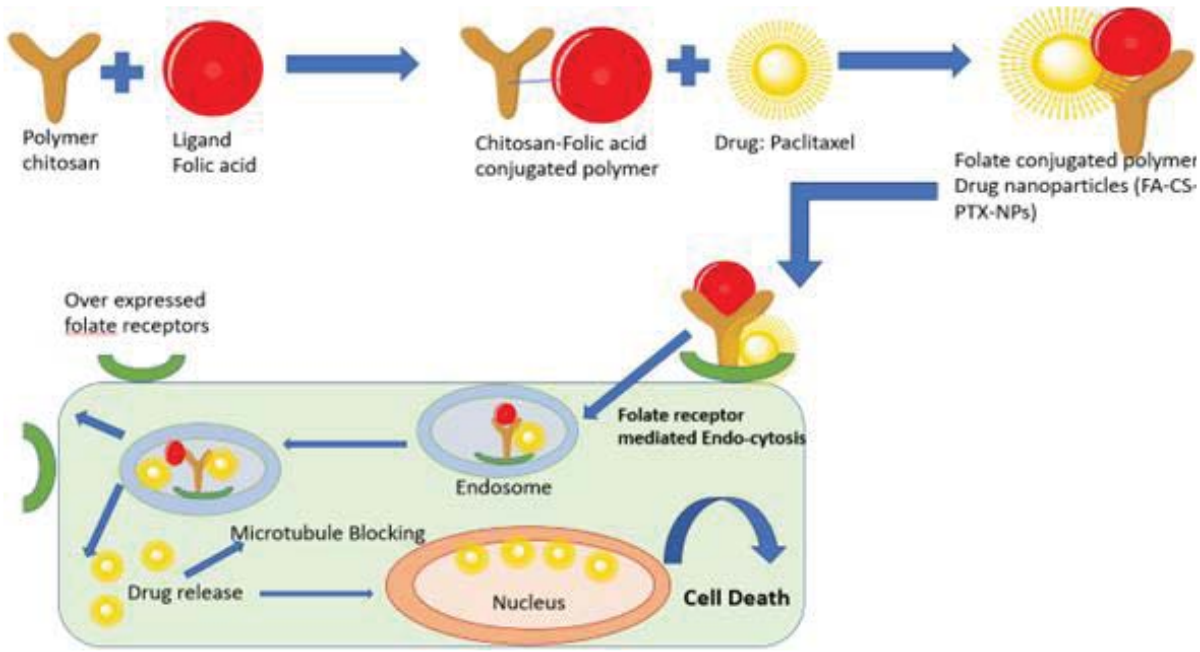

Figure 1 Strategy of drug targeting.

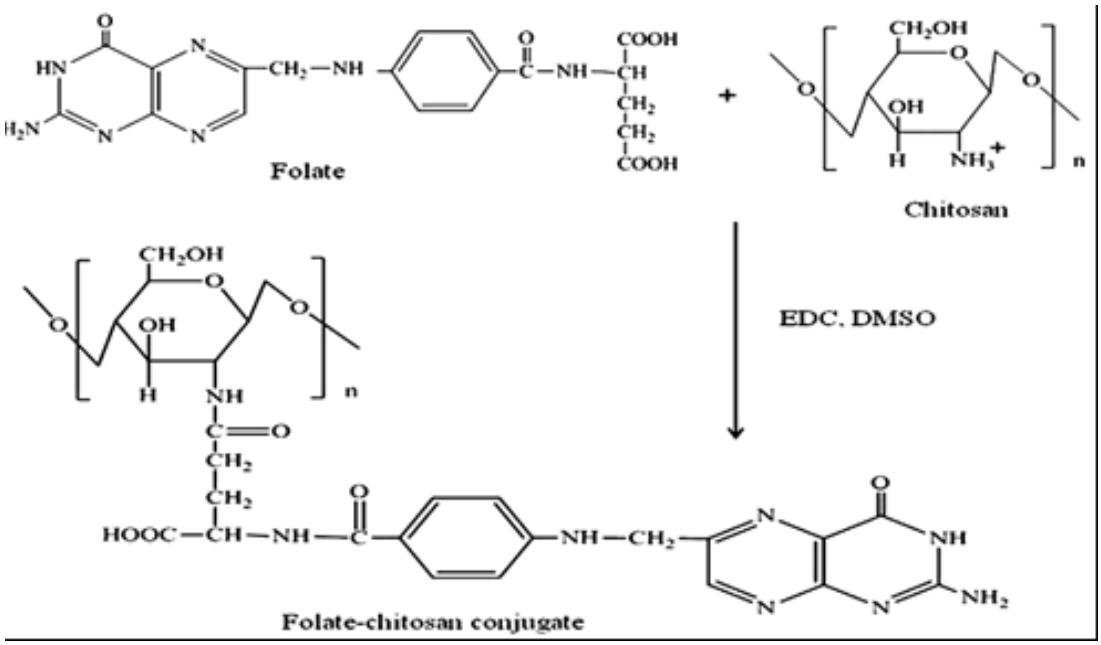

Figure 2 Chemical synthesis reaction of FA-CH conjugated polymer.

overnight. The sample was centrifuged at 10,000 rpm for 30 min to separate the supernatant, which was discarded. The resulting residue was collected and freeze-dried (Lyophilized) at -40 ˚C for 48 h. The obtained powdered nanoparticles were separated and stored in a freezer for subsequent studies [25].

Factors for formulation design: Some variables of the formulation, such as CH and STPP, were considered as variables, while the amount of drug, stirring speed, stirring time, temperature, and needle size were kept constant (Tables 1,2).

Table 1: Factors for formulation design.

S. No.	Formulation code	Variable	Variable	Constant
	FA-CH-PAC-NPs / CH-PAC-NPs	CH (mg/ml)	STPP (mg/ml)	PAC (mg)
1.	F1 / C1	1.2	1.2	50
2.	F2 / C2	1.2	0.9	50
3	F3 / C3	0.9	1.2	50

Table 2: Constant parameter for formulation design.

S. No.	Constant parameters	Amounts
1.	Drug amount	50 mg
2.	Stirring speed	1500 rpm
3.	Stirring time	2 h
4.	Temperature	25°C
5	Needle size	22 gauge

Characterization parameters

Fourier Transform Infrared (FTIR) study: Powder samples of PAC, CH, FA, FA-CH conjugate, CH-PAC-NPs, and FA-CH-PAC-NPs were analyzed through FTIR (GX-1, Perkin Elmer, USA). Samples were taken in a KBr pellet and scanned between 600 and 4000 cm-1 in the infrared spectrum.

Differential Scanning Calorimetry (DSC) study: DSC analysis was performed for PAC, CH, FA, CH-PAC-NPs, and FA-CH-PAC-NPs using a DSC (DSC 6000, Perkin Elmer, USA). One aluminum pan was filled with reference material, and another pan was filled with 10 mg samples. Samples were heated in a nitrogen environment at a rate of 10 ˚C per minute and examined in the temperature range from 0 to 300 ˚C [30].

NPs morphology study: The surface morphology of both types of NPs, i.e., the unconjugated formulation (CH-PAC-NPs) and the FA-conjugated formulation (FA-CH-PAC-NPs), was analyzed using the Transmission Electron Microscopy (TEM) method (Morgagni 268D, Fei Electron Optics, USA). Formulations were fixed using 2% phosphotungstic acid, and fixed samples were observed in a TEM at the All India Institute of Medical Sciences (AIIMS), New Delhi's Electron Microscopy Division [31].

Particle Size (PS) and Zeta Potential (ZP): A particle size analyzer (Shimadzu SALD-2201, Japan) was used to determine the average PS of the optimized unconjugated formulation and the FA-conjugated formulation. Briefly, the nanoparticulate sample dispersion was added to a distilled water-filled dispersion bath. The ZP of CH-PAC-NPs and FA-CH-PAC-NPs was assessed by zetasizer (Litesizer 500, UK). Briefly, the ZP was determined while the NPs were suspended in ultra-pure deionized water and maintained in an electrophoresis cell with an electric field of 15.24 V/cm [31].

Drug Entrapment Efficiency (EE): The 1 ml sample of each freshly prepared FA-CH-PAC-NPs and CH-PAC-NPs was accurately transferred into a centrifuge tube and was centrifuged for 45 min at 5000 rpm using a centrifuge (YJ03-0434000, Shanghai, China). Subsequently, the supernatant was separated, and free drug in supernatant was measured using Ultraviolet (UV) spectroscopy at a wavelength of 228 nm (1800, Shimadzu, Japan). To confirm potential interference, polymer solutions (Chitosan and FA-CH conjugates) without drug were scanned at 228 nm under identical experimental conditions. No significant absorbance was observed at this wavelength, indicating that the polymers did not interfere with the spectrophotometric quantification of paclitaxel. Thus, Entrapment Efficiency (EE) calculations were based solely on the absorbance corresponding to paclitaxel. Finally, the %EE of the drug in the formulation was calculated indirectly by determining the free drug in the supernatant [32]. %EE of formulations was calculated as per below equation.

$$\%EE = \frac{Total\ drug\ added - Free\ drug\ in\ supernatant}{Total\ drug\ added} \times 100$$

Drug release study

In vitro release studies were performed for

pure PTX, FA–CS–PTX nanoparticles, and CS–PTX nanoparticles was evaluated using the dialysis bag diffusion method. A dialysis membrane (MWCO = 12 to 14 kDa, Dialysis membrane-110, Himedia) was sealed at one end, equilibrated with phosphate buffer (pH 7.4), and subsequently loaded with nanoparticle dispersion equivalent to 10 mg of PTX, serving as the donor compartment. The dialysis membrane was suspended in 50 mL of phosphate buffer solution (pH 7.4), which served as the receptor compartment, and was maintained at 37 ± 0.5˚C under continuous magnetic stirring at 100 rpm to simulate physiological conditions. Samples were withdrawn at predetermined intervals ranging from 1 to 24 h, and the withdrawn volume was replaced with fresh buffer to maintain sink conditions. The samples were then spectrophotometrically examined at 228 nm, and the drug content was calculated using a standard curve [10].

In vitro cytotoxicity study of PAC and FA-CH-PAC-NPs

The cytotoxic potential of drug-loaded NPs was tested against MCF-7 cell line (purchased from the National Centre for Cell Science, Pune) using the 3-(4,5-dimethylthiazol-2-yl)-2,5-diphenyltetrazolium bromide (MTT) assay [34]. The MCF-7 cell lines were selected for cytotoxicity studies because they over-express the folate receptor in abundance and therefore MCF-7 cell lines may be the best model for testing targeting potential for folic acid-modified NPs. MCF-7 cells (10^4 cells/well) were cultured in 96-well plates and incubated for 24 h. The incubation was performed in Dulbecco's Modified Eagle Medium (DMEM) supplemented with 10% FBS and 1% antibiotic solution at 37 ˚C in a 5% CO_2 atmosphere.

Cells were exposed to several formulation concentrations the following day. After a 24 h incubation period, the cells were exposed to 250 µg/mL of MTT reagent and maintained for a further 2 h. Thereafter, 100 µL of DMSO was introduced to the cell matrix, and absorbance was recorded at 540 and 660 nm using an Enzyme-Linked Immunosorbent Assay (ELISA) plate reader. The resulting supernatant was finally removed. The IC_{50} value of the samples was estimated using GraphPad Prism software (v6). Finally, an AmScope digital camera (10 MP Aptima CMOS) was used to obtain images using an inverted microscope (Olympus ek2). All the studies were performed in triplicate (n = 3, mean ± SD).

Results and Discussion

FA was selected as a targeting ligand due to its high affinity for FR, which are frequently overexpressed on colorectal cancer cells, thereby enabling site-specific delivery of anticancer drugs [24,25]. To exploit this pathway, Chitosan Nanoparticles (CH-NPs) were synthesized via the ionic gelation method and subsequently conjugated with FA using carbodiimide chemistry. The formulations were systematically optimized by varying process parameters, including polymer-to-drug ratio, STPP concentration, and stirring speed, to achieve favorable PS, ZP, EE, and morphology. The optimized formulation parameters included a polymer concentration of 1.2 mg/mL, STPP concentration of 0.9 mg/mL, stirring speed of 1500 rpm, and crosslinking time of 2 h, which yielded stable FA–CH–PAC nanoparticles with desirable physicochemical properties.

FTIR Spectral Analysis

The purpose of the FTIR investigation was to examine the structural integrity of the functional groups found in the API in conjunction with other NP formulation components (Figure 3). Functional groups, namely N-H, C=O, H-C-H, and CONH, were represented by the different significant peaks for PAC (Figure 3a), which were obtained at 3394, 1971, 2976-2089, and 1614 cm^{-1}, respectively. Another, a peak at

1338 cm^{-1} represent the structure of the ester bond; on the other hand, the peak at 1053 cm^{-1} correspond to the C-N functional group. Moreover, the spectrum also detected some peaks of aromatic bonds like 1605, 1056, 710, and 839 cm^{-1}, however, these peaks were away from the observed peak. Thorough spectrum analysis of PAC confirmed its pure form.

For CH (Figure 3b), the broadband vibration peaks were recorded at 3699, 2880-2212, 1558, and 1320 cm^{-1} for NH/OH (stretching vibration), C-H, C=O, and C-N (amide-III oscillation), respectively. Strong absorption peaks were also detected at 1087 cm^{-1}, which is due to C-O-C vibration. The FTIR spectrum of FA (Figure 3c) exhibited intense peaks at 3910, 1694, 1605, and 1484 cm^{-1}, which are attributable to the N–H and C=O stretching of the amino group in the pteridine ring, along with C=C and C=N vibrations of FA. FA-CH conjugation was confirmed by thorough analysis of significant differences in recorded peak values of FA-CH conjugates and CH polymer (Figure 3d). A notable difference was recorded among peak values of CH as well as FA-CH. Furthermore, the absorption peak at 3910 cm^{-1} becomes more intense when the vibrations of the OH & N-H functional groups coincide. Additionally, peaks at 1694 and 1484 cm^{-1} vanished, while two new peaks were recorded at 1723 and 1012 cm^{-1}, corresponding to C-N vibration. Eventually, the absorption peak of the amide group in CH shifted from 1598 cm^{-1} to 1484 cm^{-1}, coinciding with the absorption peak of the newly created C-N bond.

Similarly, FTIR analysis of CH-PAC-NPs revealed a strong absorption band at 3394 cm^{-1} (Figure 3e), indicative of the presence of NH/OH functional groups. Moreover, the C–H stretching peaks of CH were absent in CH-PAC, while the C=O peak shifted to 1534 cm^{-1} and the C–N peak shifted to 1315 cm^{-1}, which indicates that CH-PAC-NPs were completely cross-linked and the active drug PAC was present in the formulation. The CH_2 peak of PAC disappears in the CH-PAC spectrum. On the other hand, some peaks, like 1694 cm^{-1} were replaced by 1693 cm^{-1} for CONH; a peak at 1971 cm^{-1} is replaced by 1987 cm^{-1} for C=O, and a peak at 1338 cm^{-1} is replaced by 1315 cm^{-1} for the ester bond of the CH-PAC-NPs formulation.

The strongest peak was observed at 3910 cm^{-1}/1012 cm^{-1}, for NH/OH groups in the case of the FA-CH-conjugated polymer. However, this peak was replaced by 3717 cm^{-1}/1033 cm^{-1} in formulation FA-CH-PAC-NPs (Figure 3f). In the FA-CH-PAC-NPs formulation, the PAC CH_2 peaks shifted from 2920 to 2820 cm^{-1}, the C=O peak was observed at 1972 cm^{-1}, but the C-N peak for the CONH group was not confirmed. This means that the FA-CH-PAC-NPs were slightly less cross-linked compared to the CH-PAC-NPs of the formulation and have less PAC drug incorporated compared to CH-PAC-NPs.

DSC Study

DSC was employed to confirm drug-polymer interactions in nanoparticles. Furthermore, this could help determine the melting point and extent of crystallinity of the drug in developed NPs and their components [28,33]. Figure 4 shows the DSC curves recorded for different samples, namely PAC, CH, FA, CH-PAC-NPs, and FA-CH-PAC-NPs.

PAC (Figure 4a) showed its crystalline nature, which can be confirmed by an endothermic peak corresponding to a melting point value at 220 °C. The polymer CH showed a sharp endothermic peak representing its melting point at 77.78-80.44 °C (Figure 4b). The DSC curve of ligand FA (Figure 4c) shows a characteristic peak at 163.31°C.

On the other hand, no crystalline characteristic peak of drug was detected in the formulations, suggesting that PAC exists as an amorphous form in the formulations (i.e., CH-PAC-NPs and FA-CH-PAC-NPs).

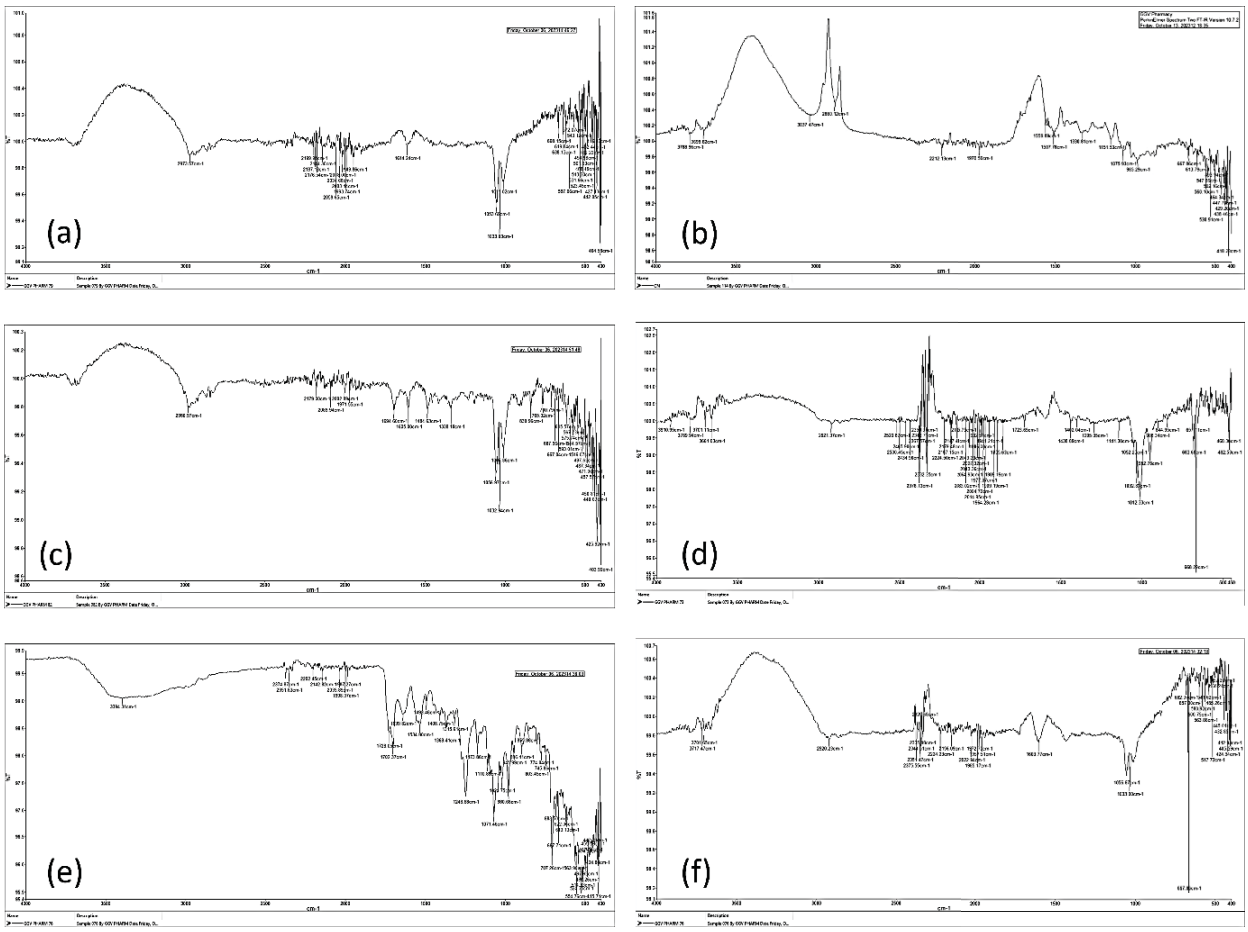

Figure 3 FTIR spectrum of (a) PAC, (b) CH, (c) FA, (d) FA-CH Conjugate, (e) CH-PAC-NPs, (f) FA-CH-PAC-NPs.

The peak of CH-PAC-NPs and FA-CH-PAC-NPs is slightly shifted to lower temperatures of 98.11 ˚C and 98.14 ˚C. It has been shown that when the drug is incorporated into NPs, the ordered position of the polymer is disturbed, which can reduce the crystallization property of drugs [27,33].

PS, ZP, and Surface Morphology

An average PS of CH-PAC-NPs was recorded to be 230 ± 6 nm, whereas the PS value of FA-CH-PAC-NPs was confirmed to be 299 ± 10 nm, as shown in table 3 and figures 5(A,B), respectively. As indicated in table 3, the Polydispersity Index (PDI) for CH-PAC-NPs and FA-CH-PAC-NPs was determined to be 0.284 ± 0.06 and 0.353 ± 0.04, respectively. The importance of the small size of NPs lies in their ability to easily evade leaky tumor vasculature and accumulate in the tumor area, where they can exert cytotoxic effects on actively growing cells [34].

The ZP of CH-PAC-NPs and FA-CH-PAC-NPs was determined to be 15.6 ± 0.7 mV and 4.9 ± 0.4 mV. However, there was a decrease in ZP when FA-CH-PAC-NPs was compared with CH-PAC-NPs (Figures 6(a,b), Table 3). After conjugation with FA, a decrease in the ZP value was also observed in other studies [35-37]. The ZP value (4.9 ± 0.4 mV) of FA-modified CH-NPs suggests

Table 3: Physicochemical characterization of CH-PAC-NPs and FA-CH-PAC-NPs (Mean ± S.D., *n* = 5).

Formulation code	Size (nm)	ZP (mV)	PDI	%Drug loading (DL)	%EE
CH-PAC-NPs	230 ± 6	15.6 ± 0.7	0.284 ± 0.06	90.21 ± 1.6	83.50 ± 2.8
FA-CH-PAC-NPs	299 ± 10	4.9 ± 0.4	0.353 ± 0.04	80.52 ± 2.4	76.50 ± 3.6

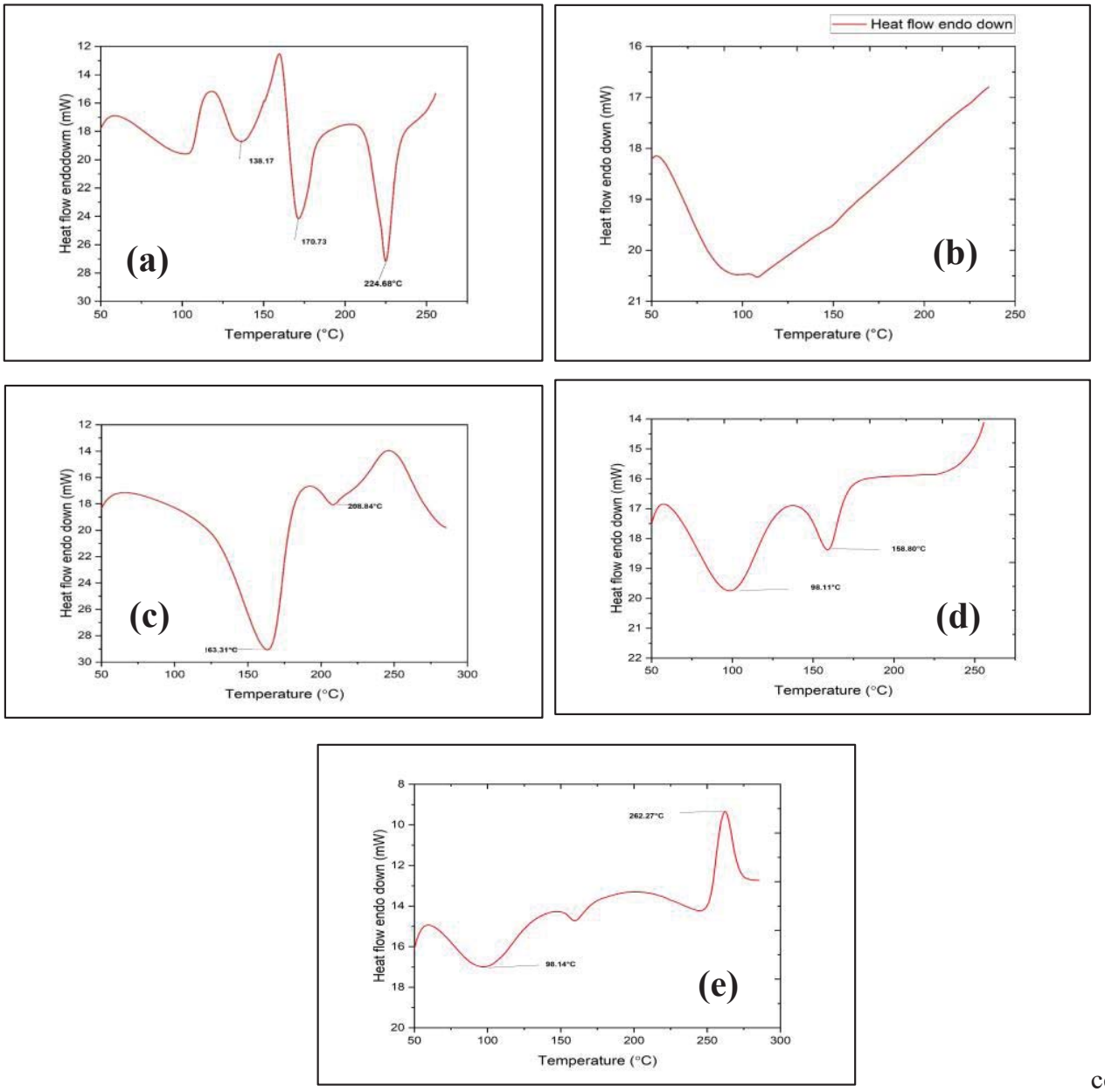

Figure 4 DSC spectrum of (a) PAC, (b) CH, (c) FA, (d) CH-PAC-NPs, (e) FA-CH-PAC-NPs.

that FA binds to CH quite strongly. The positive value could be explained by the free positive NH_2 groups present in CH molecules. The positively charged ZP facilitates passage through the negatively charged cancer cell membrane. The stability of colloidal aqueous dispersions can be predicted using the ZP value, which represents the repulsive interactions between suspended particles. TEM images of developed formulations, i.e., CH-PAC-NPs and FA-CH-PAC-NPs (Figures 7(A,B)), display smooth and spherical surfaces of the NPs. The size of FA-CH-PAC-NPs was observed to be somewhat larger than that of CH-PAC-NPs, according to TEM images.

% Drug Loading (DL) and %EE

%DL of CH-PAC-NPs and FA-CH-PAC-NPs was found to be 90.21% and 80.52%, respectively. However, the drug's EE in the formulations CH-PAC-NPs and FA-CH-PAC-NPs was found to be 76.50% and 83.50%, respectively.

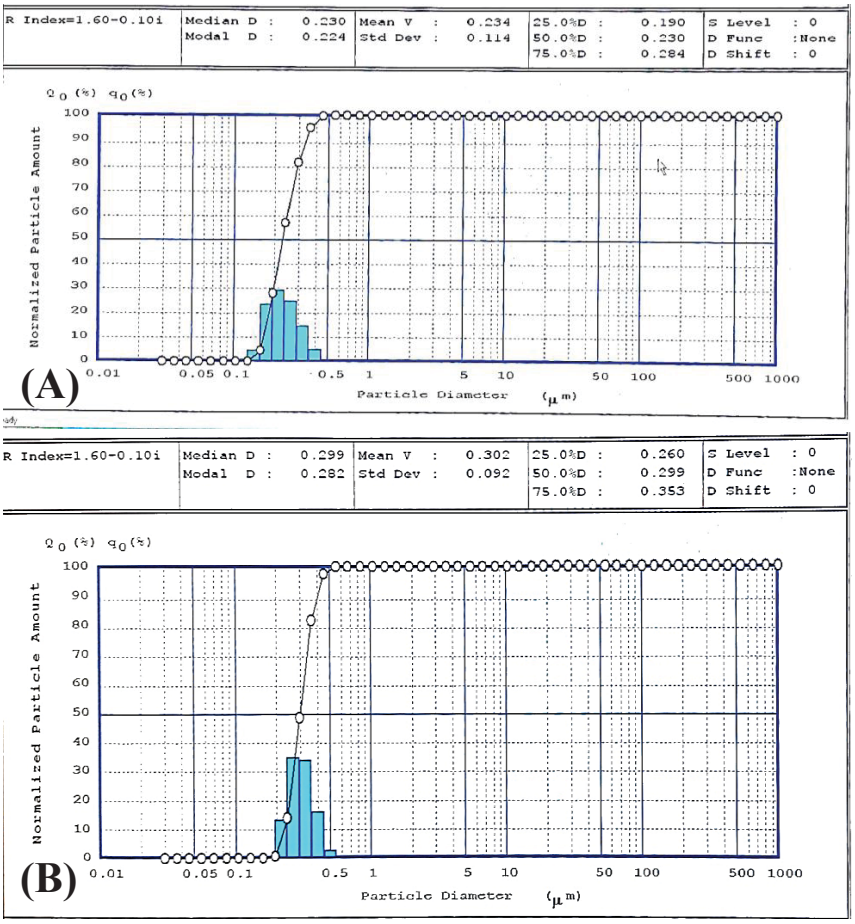

Figure 5 PS analysis of (A) CH-PAC-NPs and (B) FA-CH-PAC-NPs.

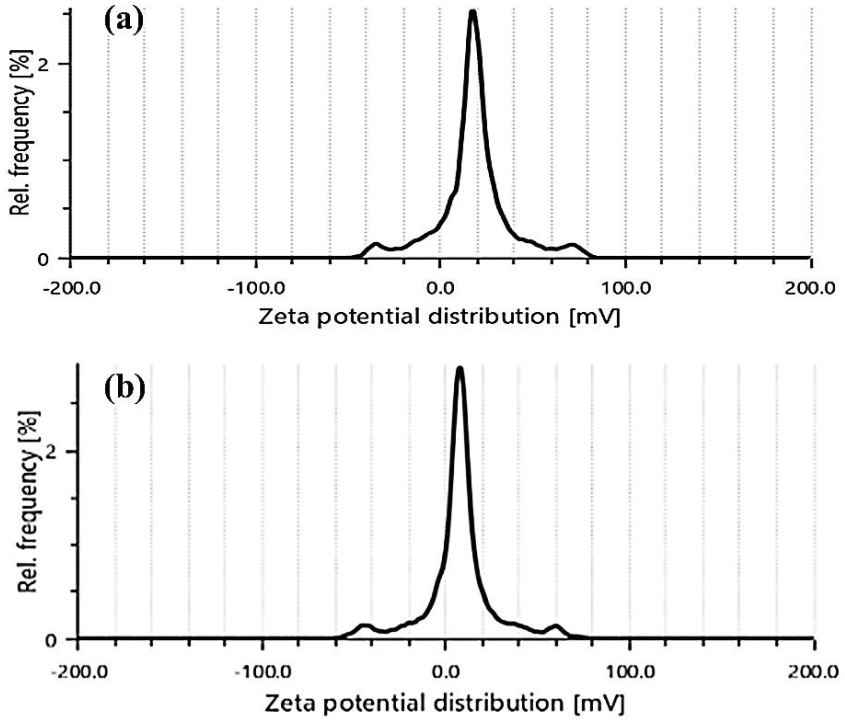

Figure 6 ZP of (a) CH-PAC-NPs, (b) FA-CH-PAC-NPs.

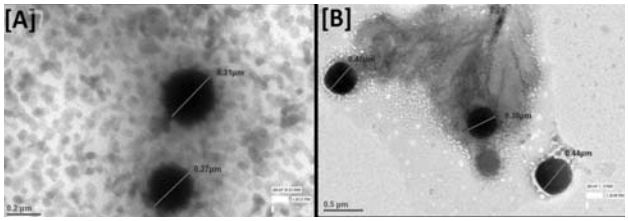

Figure 7 TEM images of (A) CH-PAC-NPs and (B) FA-CH-PAC-NPs.

Polymer solutions (Chitosan and FA–CH) showed no absorbance at 228 nm, confirming no interference in paclitaxel quantification. The addition of FA to CH molecules neutralized some of the positive charges on the amino groups. This weaker attraction between the CH and the drug resulted in a lower %EE for the NPs [38]. As a result, it was clear that the %EE was significantly influenced by the amount of FA conjugations present in the mixture (Table 3).In vitro Drug Release

PACreleasesfromdifferentnanoformulations, such as CH-PAC-NPs, FA-CH-PAC-NPs, and pure drug PAC, were measured *In vitro* at pH 7.4 using a Franz diffusion cell. The amount of PAC released after 24 h was measured, and percentages weret ale found to be 97.20%, 57.65%, and 68.88% for pure PAC, CH-PAC-NPs, and FA-CH-PAC-NPs, respectively. After the first 2 h at pH 7.4, 10.21% and 11.26% of PAC were released from CH-PAC-NPs and FA-CH-PAC-NPs, respectively. There was minimal variation in discharge pattern between these two formulations, as can be shown in figure 8. Following the first release at pH 7.4, PAC was released continuously for up to 24 h. Initial release may have been caused by weakly bound drugs on the surface of NPs.

According to these *In vitro* results, the FA-decorated NPs exhibit a typical controlled release process of PAC. The drug was discharged from the FA-conjugated NPs at a remarkably high rate, although not as fast as the pure drug [39].

In vitro Cytotoxicity

The percentage of cell death was presented in figure 9 in response to the cytotoxicity effect of two formulations, i.e., free drug (PAC) and FA-CH-PAC-NPs, against MCF-7 cells. After the

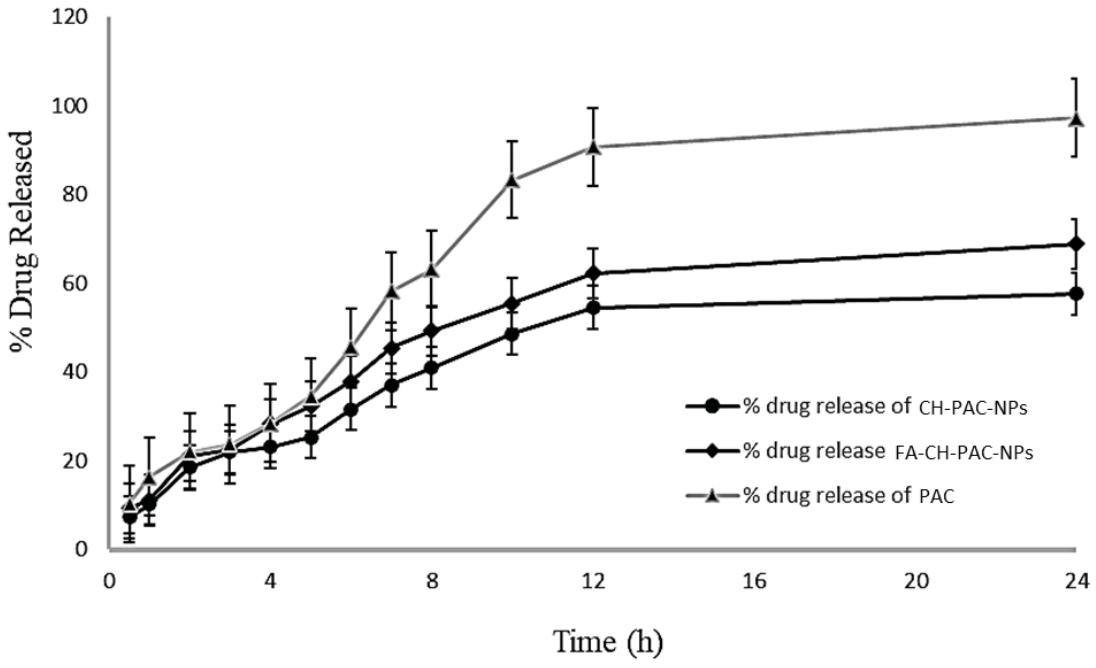

Figure 8 Release profile of drug PAC, CH-PAC-NPs, and FA-CH-PAC-NPs.

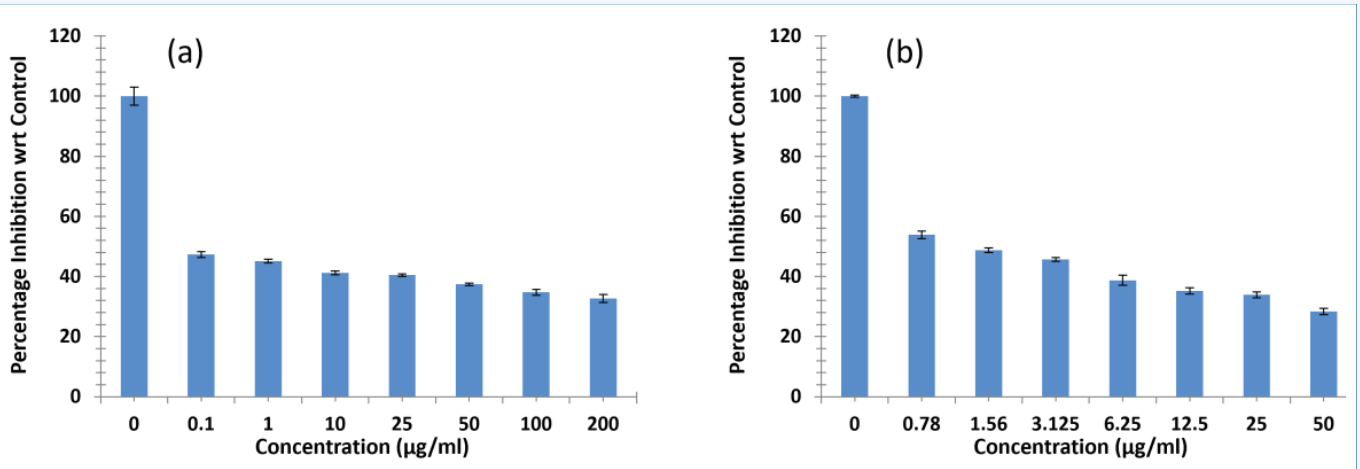

Figure 9 Graph showing percentage inhibition at different concentrations using MTT assay against MCF-7 cells. (a) PAC and (b) FA-CH-PAC-NPs.

MTT assay, findings advocated the inhibitory effect of FA-CH-PAC-NPs against MCF-7 cells was more effective compared to free PAC. The IC_{50} values, representing the concentration at which 50% of cell growth was inhibited, were 135.74 ± 0.053 µg/ml for PAC and significantly lower at 42.72 ± 0.132 µg/ml for FA-CH-PAC-NPs. This substantial reduction in IC50 values implies that the incorporation of FA enhances the anticancer efficacy of PAC. This points towards the potential of FA-CH-PAC-NPs as an effective strategy for improving therapeutic outcomes in cancer treatment.

Conclusion

10. The study successfully developed paclitaxel-loaded chitosan nanoparticles (CH-PAC-NPs) and folic acid-conjugated chitosan nanoparticles (FA-CH-PAC-NPs) utilizing the ionic gelation method. An average PS and ZP of optimized FA-conjugated formulations were 299 nm and 4.9 mV, respectively, and the excellent drug EE was 83.5%. Eventually, the % PAC released from pure PAC, CH-PAC-NPs, and FA-CH-PAC-NPs was found to be 97.20%, 57.65%, and 68.88%, respectively, after a 24 h study period. Studies of *In vitro* drug release revealed prolonged paclitaxel release; FA-CH-PAC-NPs demonstrated increased drug release at colon pH (7.4), which made them appropriate for colon-targeted delivery. The IC50 values, representing the concentration at which 50% of cell growth is inhibited, were 135.74 ± 0.053 µg/ml for PAC and significantly lower at 42.72 ± 0.132 µg/ml for FA-CH-PAC-NPs. The FA-CH-PAC-NPs demonstrated selective uptake by colon tumor cells due to FR targeting. Cytotoxicity studies revealed that FA-CH-PAC-NPs (IC_{50} = 42.72 ± 0.132 µg/ml) were more effective than free PAC (IC_{50} = 135.74 ± 0.053 µg/ml). Their ability to sustain drug release and target tumor cells makes them a potential candidate for adjunct chemotherapy in colon cancer treatment.

Funding Statement

This research was conducted without any specific financial support from public, commercial, or non-profit organizations.

References

1. Siegel RL, Miller KD, Jemal A. Cancer statistics, 2018. CA Cancer J Clin. 2018 Jan;68(1):7-30. doi: 10.3322/caac.21442. Epub 2018 Jan 4. PMID: 29313949.

2. Pajola M, Fugazzola P, Cobianchi L, Frassini S, Ghaly A, Bianchi C, Ansaloni L. Surgical Emergencies in Rectal Cancer: A Narrative Review. J Clin Med. 2024 Dec 29;14(1):126. doi: 10.3390/jcm14010126. PMID: 39797209; PMCID: PMC11721366.

3. Siegel RL, Miller KD, Wagle NS, Jemal A. Cancer statistics, 2023. CA Cancer J Clin. 2023 Jan;73(1):17-48. doi: 10.3322/caac.21763. PMID: 36633525.

4. Sung H, Ferlay J, Siegel RL, Laversanne M, Soerjomataram I, Jemal A, Bray F. Global Cancer Statistics 2020: GLOBOCAN Estimates of Incidence and Mortality Worldwide for 36 Cancers in 185 Countries. CA Cancer J Clin. 2021 May;71(3):209-249. doi: 10.3322/caac.21660. Epub 2021 Feb 4. PMID: 33538338.

5. Arnold M, Abnet CC, Neale RE, Vignat J, Giovannucci EL, McGlynn KA, Bray F. Global Burden of 5 Major Types of Gastrointestinal Cancer. Gastroenterology. 2020 Jul;159(1):335-349.e15. doi: 10.1053/j.gastro.2020.02.068. Epub 2020 Apr 2. PMID: 32247694; PMCID: PMC8630546.

6. Rawla P, Sunkara T, Barsouk A. Epidemiology of colorectal cancer: incidence, mortality, survival, and risk factors. Prz Gastroenterol. 2019;14(2):89-103. doi: 10.5114/pg.2018.81072. Epub 2019 Jan 6. PMID: 31616522; PMCID: PMC6791134.

7. Mauri G, Sartore-Bianchi A, Russo AG, Marsoni S, Bardelli A, Siena S. Early-onset colorectal cancer in young individuals. Mol Oncol. 2019 Feb;13(2):109-131. doi: 10.1002/1878-0261.12417. Epub 2018 Dec 22. PMID: 30520562; PMCID: PMC6360363.

8. Vuik FE, Nieuwenburg SA, Bardou M, Lansdorp-Vogelaar I, Dinis-Ribeiro M, Bento MJ, Zadnik V, Pellisé M, Esteban L, Kaminski MF, Suchanek S, Ngo O, Májek O, Leja M, Kuipers EJ, Spaander MC. Increasing incidence of colorectal cancer in young adults in Europe over the last 25 years. Gut. 2019 Oct;68(10):1820-1826. doi: 10.1136/gutjnl-2018-317592. Epub 2019 May 16. PMID: 31097539; PMCID: PMC6839794.

9. Rajpoot K, Jain SK. Colorectal cancer-targeted delivery of oxaliplatin via folic acid-grafted solid lipid nanoparticles: preparation, optimization, and in vitro evaluation. Artif Cells Nanomed Biotechnol. 2018 Sep;46(6):1236-1247. doi: 10.1080/21691401.2017.1366338. Epub 2017 Aug 29. PMID: 28849671.

10. Rajpoot K, Jain SK. Irinotecan hydrochloride trihydrate loaded folic acid-tailored solid lipid nanoparticles for targeting colorectal cancer: development, characterization, and in vitro cytotoxicity study using HT-29 cells. J Microencapsul. 2019 Nov;36(7):659-676. doi: 10.1080/02652048.2019.1665723. Epub 2019 Sep 18. Erratum in: J Microencapsul. 2019 Nov;36(7):I. doi: 10.1080/02652048.2019.1685169. PMID: 31495238.

11. Rajpoot K, Jain SK. Oral delivery of pH-responsive alginate microbeads incorporating folic acid-grafted solid lipid nanoparticles exhibits enhanced targeting effect against colorectal cancer: A dual-targeted approach. Int J Biol Macromol. 2020 May 15;151:830-844. doi: 10.1016/j.ijbiomac.2020.02.132. Epub 2020 Feb 13. PMID: 32061847.

12. Rajpoot K, Jain SK. 99mTc-labelled and pH-awakened microbeads entrapping surface-modified lipid nanoparticles for the augmented effect of oxaliplatin in the therapy of colorectal cancer. J Microencapsul. 2020 Dec;37(8):609-623. doi: 10.1080/02652048.2020.1829141. Epub 2020 Oct 7. PMID: 32985297.

13. Chourasia MK, Jain SK. Pharmaceutical approaches to colon targeted drug delivery systems. J Pharm Pharm Sci. 2003 Jan-Apr;6(1):33-66. PMID: 12753729.

14. Hua S. Orally administered liposomal formulations for colon targeted drug delivery. Front Pharmacol. 2014 Jun 10;5:138. doi: 10.3389/fphar.2014.00138. PMID: 24959147; PMCID: PMC4050429.

15. Pandey AN, Rajpoot K, Jain SK. 5-fluorouracil loaded orally administered wga-decorated poly(lacticco-glycolic acid) nanoparticles for treatment of colorectal cancer: In nivo evaluation. Current Nanomedicine. 2021;11:51-60. doi: 10.2174/24681873109992011231 95233.

16. Pandey AN, Rajpoot K, Jain SK. Using 5-fluorouracil-encored plga nanoparticles for the treatment of colorectal cancer: the in-vitro characterization and cytotoxicity studies. Nanomed J. 2020;7:211-24. doi: 10.22038/nmj.2020.07.0005.

17. Philip AK, Philip B. Colon targeted drug delivery systems: a review on primary and novel approaches. Oman Med J. 2010 Apr;25(2):79-87. doi: 10.5001/omj.2010.24. PMID: 22125706; PMCID: PMC3215502.

18. Sinha VR, Kumria R. Colonic drug delivery: prodrug approach. Pharm Res. 2001 May;18(5):557-64. doi: 10.1023/a:1011033121528. PMID: 11465408.

19. Rudzinski WE, Palacios A, Ahmed A, Lane MA, Aminabhavi TM. Targeted delivery of small interfering RNA to colon cancer cells using chitosan and PEGylated chitosan nanoparticles. Carbohydr Polym. 2016 Aug 20;147:323-332. doi: 10.1016/j.carbpol.2016.04.041. Epub 2016 Apr 12. PMID: 27178938.

20. Jain SK, Jain AK, Rajpoot K. Expedition of Eudragit® Polymers in the Development of Novel Drug Delivery Systems. Curr Drug Deliv. 2020;17(6):448-469. doi: 10.2174/1567201817666200512093639. PMID: 32394836.

21. Jain SK, Dubey V, Rajpoot K. D-mannose-decorated

chitosan nanoparticles for enhanced targeting of 5-fluorouracil in the therapy of colon cancer. International Journal of Pharmaceutical Sciences and Nanotechnology. 2021;14:5315-22. doi: 10.37285/ijpsn.2021.14.1.7.

22. Jain A, Jain SK, Ganesh N, Barve J, Beg AM. Design and development of ligand-appended polysaccharidic nanoparticles for the delivery of oxaliplatin in colorectal cancer. Nanomedicine. 2010 Feb;6(1):179-90. doi: 10.1016/j.nano.2009.03.002. Epub 2009 May 15. PMID: 19447205.

23. Handali S, Moghimipour E, Rezaei M, Ramezani Z, Kouchak M, Amini M, Angali KA,

24. Saremy S, Dorkoosh FA. A novel 5-fluorouracil targeted delivery to colon cancer using folic acid conjugated liposomes. Biomed Pharmacother. 2018;108:1259-73. doi: 10.1016/j.biopha.2018.09.128.

25. Bhaskaran NA, Jitta SR, Salwa, Kumar L, Sharma P, Kulkarni OP, Hari G, Gourishetti K, Verma R, Birangal SR, Bhaskar KV. Folic acid-chitosan functionalized polymeric nanocarriers to treat colon cancer. Int J Biol Macromol. 2023 Dec 31;253(Pt 5):127142. doi: 10.1016/j.ijbiomac.2023.127142. Epub 2023 Oct 4. PMID: 37797853.

26. Ullah S, Azad AK, Nawaz A, Shah KU, Iqbal M, Albadrani GM, Al-Joufi FA, Sayed AA, Abdel-Daim MM. 5-Fluorouracil-Loaded Folic-Acid-Fabricated Chitosan Nanoparticles for Site-Targeted Drug Delivery Cargo. Polymers (Basel). 2022 May 13;14(10):2010. doi: 10.3390/polym14102010. PMID: 35631891; PMCID: PMC9145180.

27. Grigoletto A, Martinez G, Gabbia D, Tedeschini T, Scaffidi M, Martin S, Pasut G. Folic Acid-Targeted Paclitaxel-Polymer Conjugates Exert Selective Cytotoxicity and Modulate Invasiveness of Colon Cancer Cells. Pharmaceutics. 2021 Jun 23;13(7):929. doi: 10.3390/pharmaceutics13070929. PMID: 34201494; PMCID: PMC8309175.

28. Kandimalla R, Aqil F, Alhakeem SS, Jeyabalan J, Tyagi N, Agrawal A, Yan J, Spencer W, Bondada S, Gupta RC. Targeted Oral Delivery of Paclitaxel Using Colostrum-Derived Exosomes. Cancers (Basel). 2021 Jul 23;13(15):3700. doi: 10.3390/cancers13153700. Erratum in: Cancers (Basel). 2025 Sep 10;17(18):2955. doi: 10.3390/cancers17182955. PMID: 34359601; PMCID: PMC8345039.

29. Koziara JM, Whisman TR, Tseng MT, Mumper RJ. In-vivo efficacy of novel paclitaxel nanoparticles in paclitaxel-resistant human colorectal tumors. J Control Release. 2006 May 30;112(3):312-9. doi: 10.1016/j.jconrel.2006.03.001. Epub 2006 Apr 19. PMID: 16626835.

30. Wan A, Sun Y, Li H. Characterization of folate-graft-chitosan as a scaffold for nitric oxide release. Int J Biol Macromol. 2008 Dec;43(5):415-21. doi: 10.1016/j.ijbiomac.2008.07.016. Epub 2008 Jul 30. PMID: 18708088.

31. Jain SK, Awasthi AM, Jain NK, Agrawal GP. Calcium silicate based microspheres of repaglinide for gastroretentive floating drug delivery: preparation and in vitro characterization. J Control Release. 2005 Oct 3;107(2):300-9. doi: 10.1016/j.jconrel.2005.06.007. PMID: 16095748.

32. Malviya R, Sundram S, Fuloria S, Subramaniyan V, Sathasivam KV, Azad AK, Sekar M, Kumar DH, Chakravarthi S, Porwal O, Meenakshi DU, Fuloria NK. Evaluation and Characterization of Tamarind Gum Polysaccharide: The Biopolymer. Polymers (Basel). 2021 Sep 7;13(18):3023. doi: 10.3390/polym13183023. PMID: 34577925; PMCID: PMC8467713.

33. Khan TA, Azad AK, Fuloria S, Nawaz A, Subramaniyan V, Akhlaq M, Safdar M, Sathasivam KV, Sekar M, Porwal O, Meenakshi DU, Malviya R, Miret MM, Mendiratta A, Fuloria NK. Chitosan-Coated 5-Fluorouracil Incorporated Emulsions as Transdermal Drug Delivery Matrices. Polymers (Basel). 2021 Sep 29;13(19):3345. doi: 10.3390/polym13193345. PMID: 34641162; PMCID: PMC8512026.

34. Dahiya M, Awasthi R, Yadav JP, Sharma S, Dua K, Dureja H. Chitosan based sorafenib tosylate loaded magnetic nanoparticles: Formulation and in-vitro characterization. Int J Biol Macromol. 2023 Jul 1;242(Pt 2):124919. doi: 10.1016/j.ijbiomac.2023.124919. Epub 2023 May 15. PMID: 37196717.

35. Gill P, Moghadam TT, Ranjbar B. Differential scanning calorimetry techniques: applications in biology and nanoscience. J Biomol Tech. 2010 Dec;21(4):167-93. PMID: 21119929; PMCID: PMC2977967.

36. Zhang HZ, Li XM, Gao FP, Liu LR, Zhou ZM, Zhang QQ. Preparation of folate-modified pullulan acetate nanoparticles for tumor-targeted drug delivery. Drug Deliv. 2010 Jan;17(1):48-57. doi: 10.3109/10717540903508979. PMID: 22747075.

37. Danhier F, Feron O, Préat V. To exploit the tumor microenvironment: Passive and active tumor targeting of nanocarriers for anti-cancer drug delivery. J Control

Release. 2010 Dec 1;148(2):135-46. doi: 10.1016/j.jconrel.2010.08.027. Epub 2010 Aug 24. PMID: 20797419.

38. Luong D, Kesharwani P, Alsaab HO, Sau S, Padhye S, Sarkar FH, Iyer AK. Folic acid conjugated polymeric micelles loaded with a curcumin difluorinated analog for targeting cervical and ovarian cancers. Colloids Surf B Biointerfaces. 2017 Sep 1;157:490-502. doi: 10.1016/j.colsurfb.2017.06.025. Epub 2017 Jun 21. PMID: 28658642; PMCID: PMC5560501.

39. Yang SJ, Lin FH, Tsai KC, Wei MF, Tsai HM, Wong JM, Shieh MJ. Folic acid-conjugated chitosan nanoparticles enhanced protoporphyrin IX accumulation in colorectal cancer cells. Bioconjug Chem. 2010 Apr 21;21(4):679-89. doi: 10.1021/bc9004798. PMID: 20222677.

40. Ramezani Farani M, Azarian M, Heydari Sheikh Hossein H, Abdolvahabi Z, Mohammadi Abgarmi Z, Moradi A, Mousavi SM, Ashrafizadeh M, Makvandi P, Saeb MR, Rabiee N. Folic Acid-Adorned Curcumin-Loaded Iron Oxide Nanoparticles for Cervical Cancer. ACS Appl Bio Mater. 2022 Mar 21;5(3):1305-1318. doi: 10.1021/acsabm.1c01311. Epub 2022 Feb 24. Erratum in: ACS Appl Bio Mater. 2023 Feb 20;6(2):932. doi: 10.1021/acsabm.2c01014. PMID: 35201760; PMCID: PMC8941513.